



**Rapport technique DEHT-DR-10/052**

**« NEXPEL Project »  
Next-generation PEM electrolyzer for sustainable hydrogen  
production**

**WP3 “New binary/ternary catalyst systems”  
Ex-situ electrocatalyst tests”**

*Authors: Edel Sheridan (SINTEF), Magnus Thomassen (SINTEF), Nicolas Guillet (CEA)*

Référence PRODEM 09.02727  
Nature du rapport Final

	Rédacteur	Vérificateur	Approbateur
Nom	Nicolas Guillet	Eric Mayousse	Olivier Lemaire
Fonction	Chercheur LCPEM	Chercheur LCPEM	Chef du LCPEM
Signature			
Date	30 juillet 2010	30 juillet 2010	30/07/2010



**LISTE DE DIFFUSION**

**Rapport complet à :**

SINTEF	E. Sheridan M. Thomassen	1 ex. (NEXPEL e-room)
Fumatech	T. Klicpera	1 ex. (NEXPEL e-room)
ISE Fraunhofer	T. Smolinka	1 ex. (NEXPEL e-room)
HELION	P. Charril	1 ex. (NEXPEL e-room)
DEHT	F. Mattera Th. Priem Secrétariat	1 ex. (Courriel) 1 ex. (Courriel) 1 ex. (Courriel)
DEHT/LCPEM	O. Lemaire J. Pauchet N. Guillet Archivage papier	1 ex. (Courriel) 1 ex. (Courriel) 1 ex. (Papier) Original + 1 ex.

**Page de garde signée + résumé + Liste de diffusion à :**

Chefs des autres départements du LITEN  
Chefs des autres laboratoires du LITEN

**Page de garde signée + résumé + Liste de diffusion + Bordereau d'envoi signé à :**

Ingénieur Qualité LITEN : J-F. NOWAK  
Bureau financier (Ventes) : M. POIRÉ



## **Résumé**

This document was produced as part of work package 3 (WP3) of the NEXPEL project (Next generation PEM electrolyser for sustainable hydrogen production), funded by European community (SP1-JTI-FCH). WP3 “New binary/ternary catalyst systems” is coordinated by SINTEF is dedicated to the development of new catalysts for oxygen and hydrogen evolution during water electrolysis.

A standardised test procedure has to be proposed for electrochemical testing of the catalysts developed.

## **Mots clefs**

**ÉLECTROLYSE DE L’EAU, ELECTROLYSE PEM, NEXPEL, CATALYSEUR, PROTOCOLE DE TEST**



<b>I.</b>	<b>INTRODUCTION</b> .....	<b>5</b>
I.1	STANDARDISED DATA AND STATE OF THE ART COMPARISON OF WATER ELECTROLYSERS .....	6
I.2	TARGETED RESULTS WITHIN NEXPEL PROJECT.....	6
<b>II.</b>	<b>THEORY OF ANALYTICAL TECHNIQUES</b> .....	<b>7</b>
II.1	CYCLIC VOLTAMMETRY .....	7
II.1.1	<i>Cyclic Voltammetry of noble metal based materials</i> .....	7
II.1.2	<i>Cyclic Voltammetry of oxides</i> .....	10
II.2	LINEAR SWEEP VOLTAMMETRY - POLARISATION CURVES.....	12
<b>III.</b>	<b>EXPERIMENTAL</b> .....	<b>13</b>
III.1	SAMPLE PREPARATION.....	13
III.1.1	..... <i>Catalyst layer preparation</i>	13
III.1.2	..... <i>MEA preparation</i>	13
III.2	THREE ELECTRODE CELL SETUP .....	15
III.2.1	..... <i>Flat electrode</i>	15
III.2.2	..... <i>Rotating ring – disc electrode</i>	16
III.3	MEA TESTING DEVICES.....	17
III.3.1	..... <i>Half cell setup</i>	17
III.3.2	..... <i>Easy Test Cell</i>	18
III.3.3	..... <i>Small size electrolysis cell</i>	20
<b>IV.</b>	<b>TESTING PROTOCOLS</b> .....	<b>21</b>
IV.1	THREE ELECTRODE CELL SETUP .....	21
IV.2	SAMPLE PREPARATION.....	22
IV.2.1	..... <i>Deposition of catalyst suspension</i>	22
IV.2.2	..... <i>Catalyst ink</i>	22
IV.2.3	..... <i>MEA</i>	22
IV.3	CHARACTERIZATION TECHNIQUES.....	23
IV.3.1	..... <i>Cyclic voltammetry – Active surface Area</i>	23
IV.3.2	..... <i>Cyclic Voltammetry - Polarisation curves</i>	23
IV.4	IMPEDANCE SPECTROSCOPY MEASUREMENTS.....	26
IV.5	STABILITY CRITERIA (HALF CELL AND SINGLE CELL TESTS).....	27
IV.6	POLARISATION CURVE (SINGLE CELL TESTS).....	28
<b>V.</b>	<b>REFERENCES</b> .....	<b>30</b>



## I. Introduction

This document was produced as part of WP3 of the NEXPEL project (Next generation PEM electrolyser for sustainable hydrogen production), funded by European community (SP1-JTI-FCH). WP3, coordinated by SINTEF is dedicated to the development of new catalysts for oxygen and hydrogen evolution during water electrolysis.

A standardised test procedure has to be proposed for electrochemical testing of the catalysts developed.

- Reaction occurring at the cathodic side of a PEM water electrolyser is expected to be the reduction of protons ( $H^+$ ):



Catalysts used for this electrode are mainly composed of platinum (Pt) on a support material. Platinum black or carbon supported platinum nanoparticles can be used. Platinum loading is generally comprised between 0.4 and 5mg Pt  $cm^{-2}$ .

- At the anodic side, the reaction of water oxidation is supposed to be:



Due to high potential and low pH of the proton exchange membrane, only few metal oxides are stable and can be used as catalysts. Iridium (Ir) based multimetallic (with Ru, Ta, Sn...) oxides are usually utilized with loadings comprised between 1 and 6 mg<sub>IrO<sub>2</sub></sub>  $cm^{-2}$ .

Devices used to evaluate the electrocatalytic performance of anodic and cathodic catalysts would not be exactly the same. For the anodic side, catalysts would have to be set on a support that doesn't oxidize at potentials that could reach 1.5 V vs. RHE.



### ***1.1 Standardised data and state of the art comparison of water electrolysers***

Generally when comparing catalysts for water electrolysis a number of parameters are considered including the catalyst activity in relation to surface area, the noble metal loading, stability and durability. In addition structural analysis is also often reported.

The electrochemically active surface area of the catalyst material which is generally determined by cyclic voltammogram measurements and analysis.

Techniques such as XRD, BET, SEM and EDX are often employed for structural analysis of the catalysts.

### ***1.2 Targeted results within NEXPEL project***

- H<sub>2</sub> evolution catalysts: Despite the development of supported noble metal catalysts for PEM fuel cells little implementation of such catalysts has been seen for water electrolysis. Generally Platinum Black has been used with a loading of up to 2 mg cm<sup>-2</sup>. Within the Nexpel project it is expected to reduce Pt loading to 0,2 mg cm<sup>-2</sup> by using Pt on a support material such as carbon.
- O<sub>2</sub> evolution catalysts: Ru or Ir metal / metal oxides often for agglomerates and hence the active material in its pure form is not being used to its full potential. A relatively high loading of 6 mg cm<sup>-2</sup> of Ir or Ru eg. Ir black is used. Supported Ir or Ir oxide provides a cheaper alternative and the targeted loading within the Nexpel project is 0,8 mg cm<sup>-2</sup>.



## II. Theory of Analytical Techniques

### II.1 *Cyclic Voltammetry*

Cyclic voltammetry (CV) is one of the most useful analysis tools for investigating electrocatalysts. The voltammogram is a current response to a potential sweep and gives an electrochemical spectrum of the electrode surface, with information regarding the solid-state redox transitions, active area and the electrode capacitance being found. Normally, cyclic voltammetry is performed by sweeping the potential between two potential limits at a constant sweep rate (linear cyclic voltammetry).

Often cyclic voltammetry is used to study electrode reactions involving electroactive species present in the electrolyte, but it is also extremely useful for following the adsorption of species on the electrode (e.g. H<sub>ads</sub> or CO on Pt). Reversible adsorption processes are characterised by the anodic and cathodic peaks being sharp and symmetrical with no significant difference in the peak potentials. For irreversible adsorption processes, the forward peak (i.e. adsorption of soluble species onto the electrode) becomes non-symmetric and the reverse desorption peak does not occur. For quasi-reversible reactions, there will be both peaks, however they will not be symmetric and there will be some difference between the peak potentials.

#### II.1.1 Cyclic Voltammetry of noble metal based materials

Noble metals such as Pt, Pd and Au have well defined hydrogen adsorption and desorption peaks seen upon cycling between suitable potential limits using the cyclic voltammetry technique. Due to these defined peaks several values can be determined for the Pt based catalysts. By analysis of the oxidation peaks a determination of the electroactive surface area (EAS) of catalyst ( $\text{m}^2 \text{g}^{-1}_{\text{catalyst}}$ ) can be determined.

The EAS areas can be calculated from the hydrogen desorption peak area and from the CO stripping peak area.

Figure 1 shows the cyclic voltammograms obtained in 1 M H<sub>2</sub>SO<sub>4</sub> at 298 K and 20 mV s<sup>-1</sup> scan rate on Pt/C, PtPd/C and Pd/C catalysts <sup>[1]</sup>.

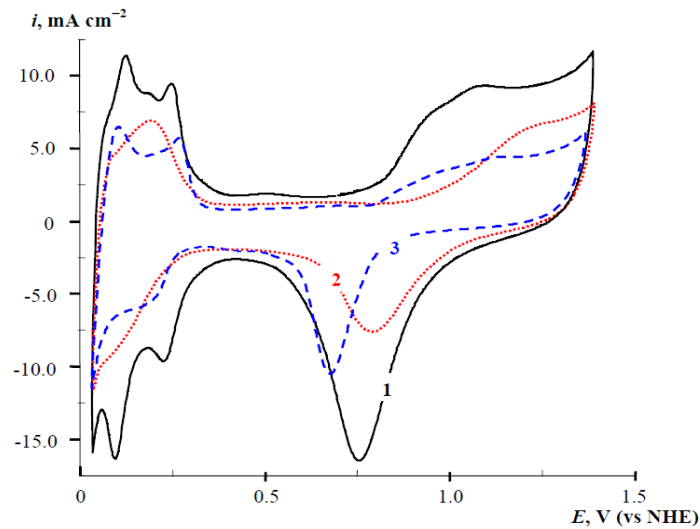


Figure 1: Cyclic voltammograms (20 mV s<sup>-1</sup>) of electrodes based on synthesized catalyst. 1 – Pt40/Vulcan-XC72, 2 – Pt1Pd140/Vulcan-XC72 and 3 – Pd40/Vulcan-XC72. <sup>[1]</sup>

The EAS are calculated by measuring the peaks area in the voltammograms and using the following equations:

$$EAS_{H_{upd}} = \frac{Q_H (\mu C)}{210 (\mu C.cm^{-2})} = \frac{A_H / v}{210}$$

$A_H$  is the hydrogen peak desorption area (C.V.s<sup>-1</sup>),  $v$  the scan rate (mV.s<sup>-1</sup>) and 210  $\mu C cm^{-2}$  is an estimated value of the adsorption charge of an hydrogen monolayer on a smooth platinum electrode <sup>[2,3,4,5,6]</sup>.

Additionally to know and quantify the electrochemical active area in catalytic systems based on Pt, carbon monoxide is a useful probe in electrochemical platinum based catalysts characterization, blocking the Pt surface at low potentials (hydrogen region). The CO stripping procedure involves a electrochemical adsorption of carbon monoxide followed by electrooxidation.

Figure 2 shows the first and the last cyclic voltammograms recorded on Pt/C catalyst in 0.5M H<sub>2</sub>SO<sub>4</sub> at 298 K and 20 mV s<sup>-1</sup> scan rate after CO adsorption on catalyst and illustrates the charges corresponding to desorption of H<sub>upd</sub> ( $Q_H$ ) and CO ( $Q_{CO}$ ).

The amount of CO adsorbed its estimated by stripping peak integration corrected to electric double layer assuming that one CO monolayer its adsorbed linearly and the charge used for oxidise its 420  $\mu C cm^{-2}_{Pt}$ . <sup>[7,3,8,9,10]</sup>





$$EAS_{CO} = \frac{Q_{CO}(\mu C)}{420(\mu C.cm^{-2})} = \frac{A_{CO}/V}{420}$$

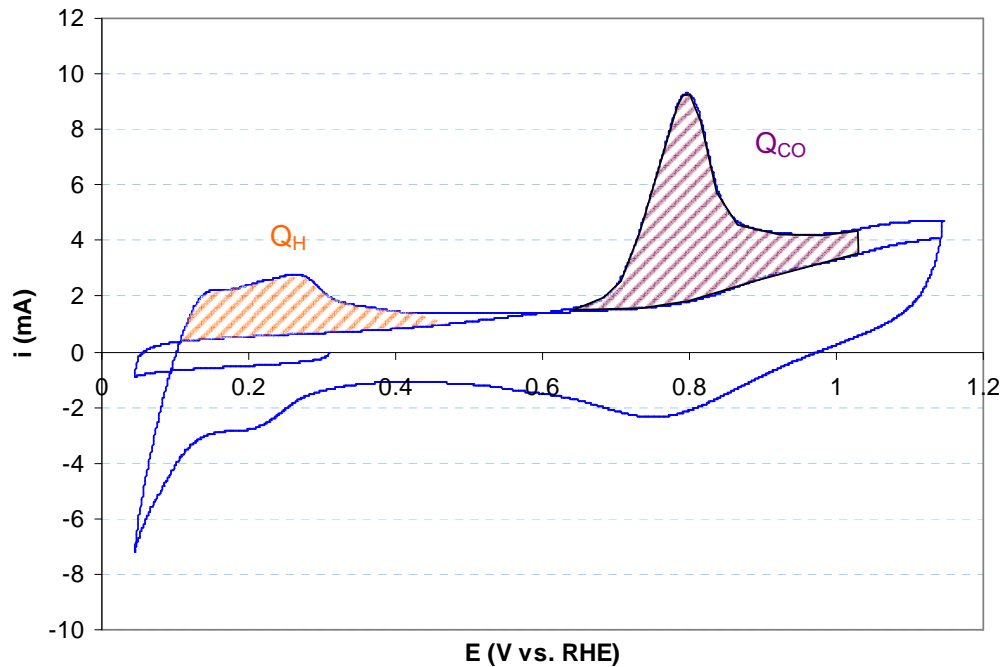


Figure 2: Cyclic voltammetry of a Pt/C catalyst – measurement of  $Q_H$  corresponding to  $H_{upd}$  desorption en  $Q_{CO}$  corresponding to CO oxidation

CO stripping shape in Pt catalyst are conditioning by morphology, structure, size and chemical nature, give us additional information about how the particles are supported on, if they are aggregated or homogeneously disperse <sup>[10,11]</sup>.

Among others, CO Stripping evaluate tolerance towards carbon monoxide in electrocatalysts ( $H_2/CO$  supply from reformat), electrode activity in organic molecules electrooxidation since CO it's an intermediate produced during electrooxidation which pass through by successive deprotonation at room temperature <sup>[12]</sup>.



### II.1.2 Cyclic Voltammetry of oxides

Noble metal oxides such as IrO<sub>2</sub> and RuO<sub>2</sub> have quite characteristic voltammograms in acid electrolyte<sup>[14,13]</sup> as shown by Figure 3.

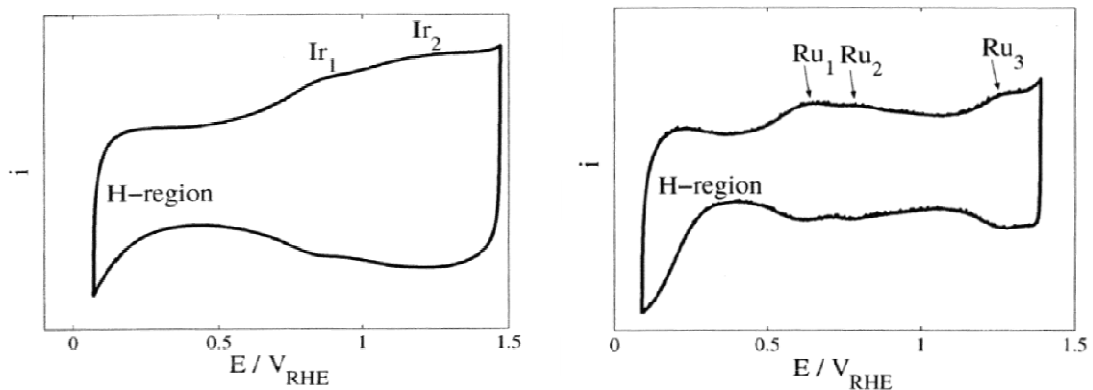
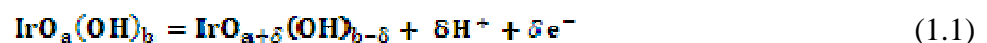


Figure 4: Cyclic voltammogram of IrO<sub>2</sub> and RuO<sub>2</sub><sup>[14]</sup>

The voltammograms show the solid state redox transitions as peaks or broad waves. These redox transitions occur due to the adsorption and oxidation of oxygenated species from the electrolyte. These processes can be described as a pseudo capacitance, as the adsorbed species effectively store charge on the electrode surface. This differs from the double layer capacitance as this pseudo capacitance is a Faradaic process in which electrons cross the double layer region.

The charging / adsorption process for iridium oxide is given by the following equation (1.1):



Normally the peaks found on a voltammogram of iridium oxide in acid are located around 0.8-0.9 and 1.25-1.35 V and correspond to the redox transitions of Ir<sup>3+</sup>/Ir<sup>4+</sup> and Ir<sup>4+</sup>/Ir<sup>6+</sup> respectively.

Similarly to IrO<sub>2</sub>, the charging process for RuO<sub>2</sub> is given by (1.2):



This charging process is associated with three redox transitions, Ru<sup>2+</sup>/Ru<sup>3+</sup>, Ru<sup>3+</sup>/Ru<sup>4+</sup> and Ru<sup>4+</sup>/Ru<sup>6+</sup> resulting in three broad peaks in the oxide region of the voltammogram (Figure 4).

At higher potentials ruthenium oxide electrodes can be further oxidised to Ru<sup>8+</sup>, which can result in formation of volatile RuO<sub>4</sub>.



$\text{IrO}_2$  and  $\text{RuO}_2$  both are covered in a hydroxide layer when placed in an electrolyte. This hydroxide and lattice oxy groups enable the oxides to conduct protons via a "hopping" type mechanism. This implies that under some circumstances, protons can penetrate into the bulk of the oxide along crystal grain boundaries, pores, and defects, with the transport limited by the diffusion at these interfaces.

The ratio of  $Q_a/Q_c$  is used to examine the reversibility of the redox process, which is attained by calculating the ratio of the charge between 0.15 and 1.15 V vs. SCE of the forward sweep and the reverse sweep <sup>[15,16,17,18]</sup>. These calculations could show changes in the reversibility during the charging process.

To estimate the EAS of the electrodes, the adsorption of  $\text{Zn}^{2+}$  ions onto the electrode surface, used by Kozawa et al. <sup>[19]</sup> on  $\text{IrO}_2$ , O'Grady et al. <sup>[20]</sup> on  $\text{RuO}_2$  and Savinell et al. <sup>[21]</sup> on both catalysts.

The electrode was placed in a Plexiglas adsorption cell and immersed in a solution of 0.5M  $\text{NH}_4\text{Cl}$  and 0.001M  $\text{ZnO}$ . Concentration of  $\text{Zn}^{2+}$  rapidly decreases during the first 2.5h of immersion, then adsorption onto the catalysts was supposed to be complete after 16h. The amount of  $\text{Zn}^{2+}$  ions adsorbed was determined by titration with 0.00025M EDTA using Erichrome Black T as an indicator. Assuming an area of 1.7  $\text{nm}^2$  per adsorbed  $\text{Zn}^{2+}$  ion, the EAS of the electrode was then calculated.

The use of voltammetric charge to estimate EAS of ruthenized titanium surfaces was investigated by Burke et al. <sup>[22]</sup> and used by Savinell et al. <sup>[21]</sup>. The electrodes were immersed in 1M  $\text{H}_2\text{SO}_4$  in a test cell where the working electrode was placed between two parallel DSA counter electrodes. A standard calomel electrode (SCE) with a Luggin probe was employed as the reference. A triangular voltage wave was applied at a sweep rate of 20  $\text{mV s}^{-1}$  in the potential range of 0.05 - 1.0 V vs. SCE. These conditions were reported to give reproducible charge for catalysts. The steady-state voltammograms were recorded and anodic and cathodic charges were measured.

Savinell et al. <sup>[21]</sup> found that the electrochemically accessible surface area was an apparent linear function of voltammetric charge for  $\text{RuO}_2$  up to a loading of 14  $\text{mg cm}^{-2}$ , giving a correlation of  $2643 \pm 186 \text{ cm}^2 \text{ C}^{-1}$ . Another correlation was found for  $\text{IrO}_2$  films ( $3260 \pm 174 \text{ cm}^2 \text{ C}^{-1}$ ) up to a loading of 2.66  $\text{mg cm}^{-2}$ . However, some doubt about the validity of the latter correlation remains since its use in measuring kinetic rate constants of a simple redox reaction gives values that are an order of magnitude lower than expected.

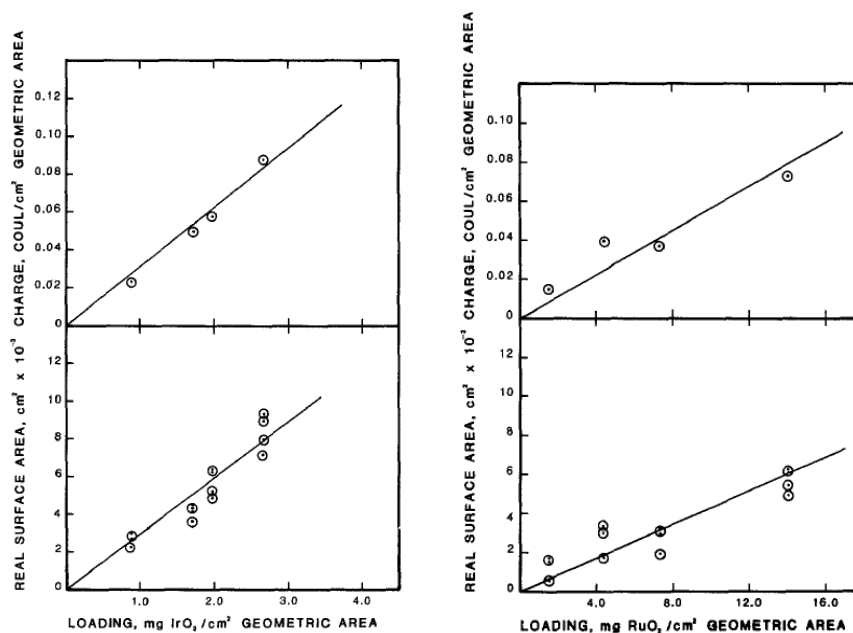


Figure 5: Voltammetric charge and electrochemically active (real) surface area correlated with loading for IrO<sub>2</sub> and RuO<sub>2</sub> - coated titanium electrodes. [21]

## II.2 Linear Sweep Voltammetry - Polarisation curves

Linear Sweep Voltammetry examines the potential–current (E-I) relationship at the electrode surface and can be carried out under either potentiostatic (controlled potential) or galvanostatic (controlled current) conditions in which the response in the current or potential is monitored. In order to obtain a steady state the scan is usually run very slowly typically 2 – 5 mV s<sup>-1</sup>. The analysis of the polarisation curve can provide information concerning the kinetics and the mechanism of the reaction at the catalyst in addition to providing a useful tool to compare catalyst activity.



### III. Experimental

#### III.1 *Sample preparation*

##### III.1.1 Catalyst layer preparation

In most cases, the catalyst is mixed with deionised water, isopropanol and ionomer (Nafion or others...). Amount of ionomer can vary: 16wt.% to 30wt.% [23,24]. After sonication and/or magnetic stirring, the obtained ink is painted or sprayed on a conductive substrate [25,26].

Titanium-based substrates are typically used for anodic catalysts. They could be polished and etched in concentrated HCl at 80°C [21,27].

Catalyst layer is sometimes directly grown on the surface of a conductive substrate such as titanium foil or sinter, directly [28,29] or after sand-blasting and etching into boiling 10% oxalic acid [30], boiling 37% HCl [31] or both [32,33].

Catalyst can also be electrodeposited on the surface of a conductive electrode (glassy carbon, Au, Pt) [34], ITO [35] or other conductive layers [36,37].

##### III.1.2 MEA preparation

The powder of catalyst is usually mixed with Nafion ionomère in alcoholic solution (5wt.% [38,39], 10wt.% [40,41], 15wt.% [42], 20wt.% [43], 25wt.% [44], 30wt.% [45,46], 33wt.% Nafion [47,48,49,50]), then sprayed onto a Nafion (112 to 117) membrane by spray or decal [40,39,51] technique.

Ma et al. [46] made an interesting study and found that the Nafion content in the catalyst layers has an obvious influence on the PEMWE performance. In particular, there is a significant decrease when the Nafion content is relatively high, such as 40wt.%.

It is ascribed to relatively thick Nafion film coating on catalyst surface that increases resistances of mass transportation, charge transfer and ionic transfer. The proton conductive resistance changed with operating conditions but it was clearly seen that the resistance enhances with the increasing of Nafion content. On the other hand, too low content of Nafion in catalyst layer can reduce three-phase interface and decrease the adhesive force between catalyst layer and membrane.

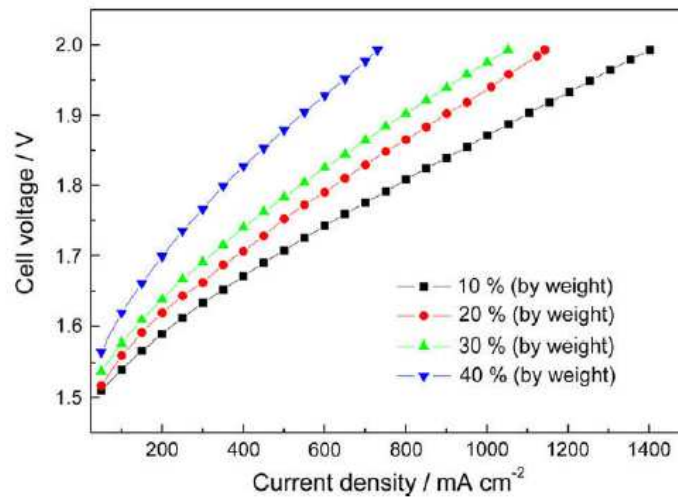


Figure 6: effect of Nafion contents in catalyst layer of anodes on the PEMWE performance<sup>[46]</sup>

The low adhesive force will lead to an easy breaking away of the catalyst layers from the surface of membrane. In order to ensure the stability of MEA, the best content of Nafion in the anode was about 30wt.%.



### III.2 Three electrode cell setup

The three electrodes cell setup is the most common setup used in electrochemistry. It is composed of a working electrode (WE) counter electrode (CE) and reference electrode (REF) immersed in an electrolyte. Electrolyte is generally an aqueous solution of  $H_2SO_4$  or  $HClO_4$ .

#### III.2.1 Flat electrode

- Principle:

It is the simplest setup. Electrodes are prepared by immobilizing the catalyst on the surface of a flat metallic electrode. This electrode is then immersed in the electrolyte of a three electrodes electrochemical setup (working electrode WE, counter electrode CE and reference electrode REF). Electrolyte is generally an aqueous solution of  $H_2SO_4$  or  $HClO_4$ .

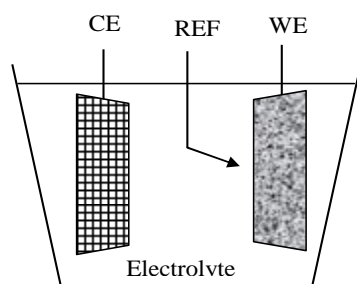


Figure 7 : flat electrode principle

- Catalyst layer: see [Catalyst layer preparation](#)

The catalyst layer is composed of a catalyst powder set in suspension in a solvent (water, ethanol, isopropanol...). This suspension can be sprayed or deposited on the flat electrode to fully cover it. After drying, a binder as Nafion solution is then generally added on the catalyst to avoid the catalyst to peel off.

The catalyst can also be set in suspension in a mixture of solvent and binder. The support is then coated with an appropriate amount of this mixture.

Advantage	Disadvantage
<ul style="list-style-type: none"> <li>- easy to implement</li> <li>- small amount of catalyst needed (depend on the WE surface area)</li> </ul>	<ul style="list-style-type: none"> <li>- The catalyst support has to be stable throw the whole potential window of measurement (0 to 1.5V vs. RHE). It could be a titanium plate or a gold plate.</li> <li>- Evacuation of produced gas</li> <li>- Representative of MEA behaviour?</li> </ul>

### III.2.2 Rotating ring – disc electrode

- Principle:

The principle of rotating ring disc electrode is more or less the same as the flat electrode. The catalyst is immobilized on the surface of a flat metallic electrode. This electrode is immersed in the electrolyte of a three electrodes electrochemical setup. Glassy carbon or gold disks (Pine Instruments) is used as a substrate for the electrocatalysts.

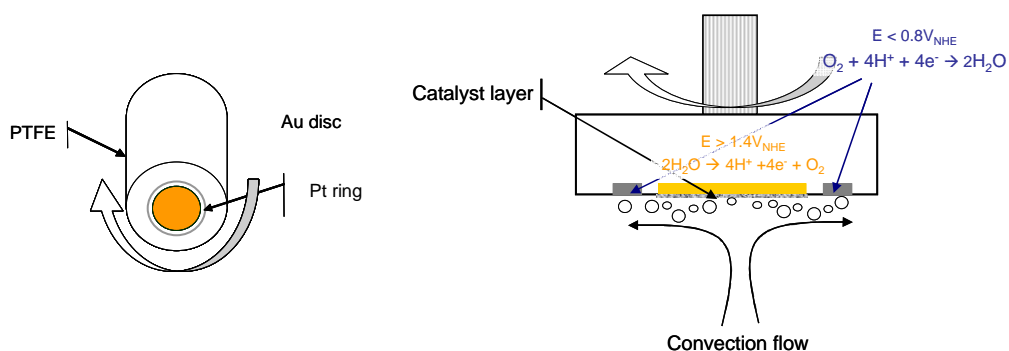


Figure 8 : Rotating ring disc electrode

Main difference is that the electrode rotates at a define speed allowing a convection flow of electrolyte that evacuate gas by the electrode sides.

A part of the produced gases can be collected on the ring. When setting the potential of the ring at fixed value, the current read is proportional to the produced gas flow.

- Catalyst layer:

As before, the catalyst suspension can be sprayed or deposited on the flat electrode to fully cover it, then followed by a Nafion solution binder deposition. Or the electrode can be coated with a suspension of catalyst in a mixture of solvent and binder.

Advantage	Disadvantage
<ul style="list-style-type: none"> <li>- easy to implement</li> <li>- small amount of catalyst needed</li> <li>- measurement of the produced gas flow while cycling potential</li> </ul>	<ul style="list-style-type: none"> <li>- The catalyst support has to be stable throw the whole potential window of measurement (0 to 1.5V vs. RHE). It could be a gold plate.</li> <li>- Representative of MEA behaviour?</li> </ul>





### III.3 MEA testing devices

Three different devices can be used to evaluate and compare the electrocatalytic performance of the catalyst. Each device has got its advantages and disadvantages. We'll present them and discuss their utilization for the electrocatalysis testing.

#### III.3.1 Half cell setup

- Principle:

The “half cell” device was developed to test the electrocatalytic activity of the catalysts layer assembled with a proton exchange membrane. The catalyst layer is set between a gas diffusion layer and the membrane; we obtain a membrane – electrode assembly. Only one catalytic layer is deposited on one side of the membrane. The other stay blank.

This assembly is put in a sample holder comprising a current collector (gold) and the membrane side is set in contact with the electrolyte of a three electrodes electrochemical setup. Produced gases are evacuated through the gas diffusion layer.

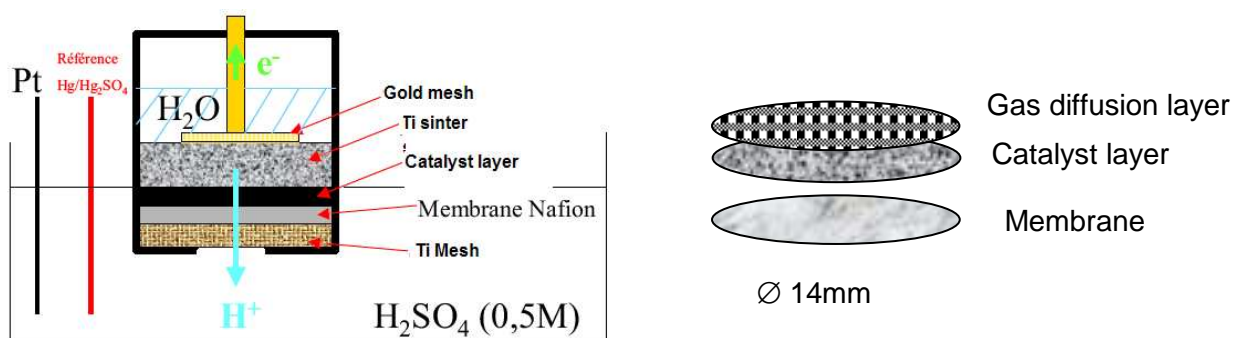


Figure 9 : half cell setup

- Sample preparation: see [MEA preparation](#)

A suspension of catalyst in a mixture of solvent and binder is deposited on the membrane (spray, knife coating, screenprinting, decal ...) or on the gas diffusion layer. It is possible to evaluate the influence of catalyst layer composition (amount of Nafion) and differences relative to the deposition technique.

Advantage	Disadvantage
<ul style="list-style-type: none"> <li>- easy to implement</li> <li>- small amount of catalyst needed</li> <li>- representative of MEA behavior</li> </ul>	<ul style="list-style-type: none"> <li>- High electrical resistance of electrolyte (few <math>\Omega \text{ cm}^{-2}</math>) leading to a limitation to low currents densities</li> </ul>

### III.3.2 Easy Test Cell

The easy test cell concept has been developed by Radev et al. [52]. It allows testing and optimizing single electrodes before coupling them to a working cell.

- Principle:

The counter electrode is used to pass a current through the working electrode. The EasyTest approach offers the possibility for carrying out electrochemical tests of MEA sealed in one gas compartment. Thus, instead of two different reactions proceeding on both electrodes, the reaction on the CE will be the same as that on the WE but will proceed in the opposite direction.

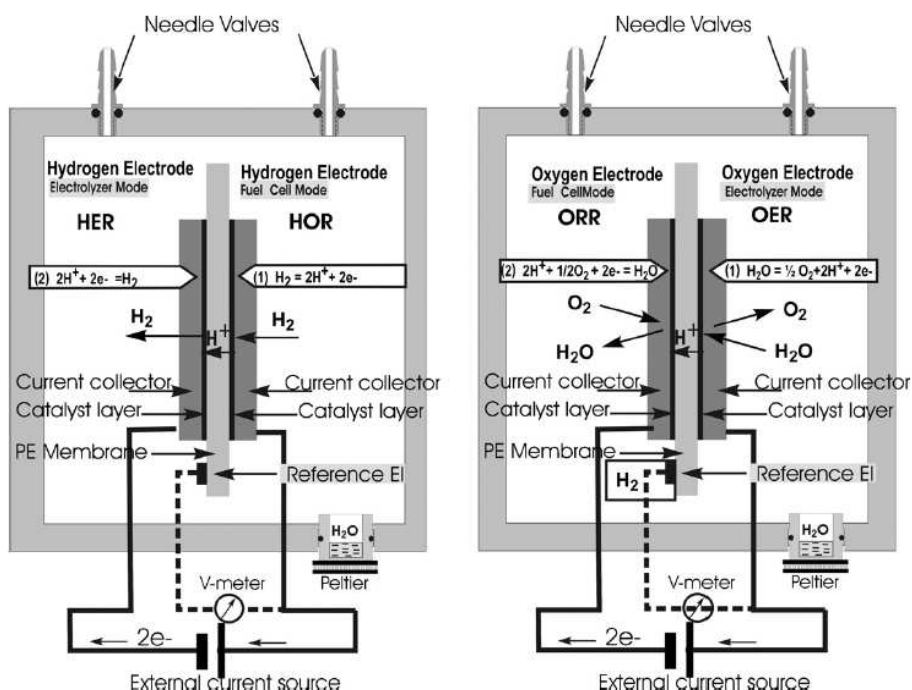


Figure 10: The EasyTest Cell principle – hydrogen version (left) and oxygen version (right). [52]

A counter electrode containing an active catalyst toward the opposite reaction is a prerequisite for this case.

- Example of results:

With such a device, it is possible to perform polarisation curves and cyclic voltammetry and compare them to those obtained on a PEMWE.

Experiments were performed on a MEA prepared by hot pressing of catalyzed gas diffusion layers on both sides of a Nafion117 membrane. The catalysts – Pt, IrOx, and a composite

IrOx/Pt/IrOx – were deposited directly on the Toray paper gas diffusion sheets by dc magnetron sputtering. In order to improve the adherence of the catalytic layer to the substrate and, eventually, to prevent the oxidation of the carbon paper during oxygen evolution in the PEM WE, all films were deposited on a  $7.5 \mu\text{g cm}^{-2}$  (50 nm thick) Ti sublayer.

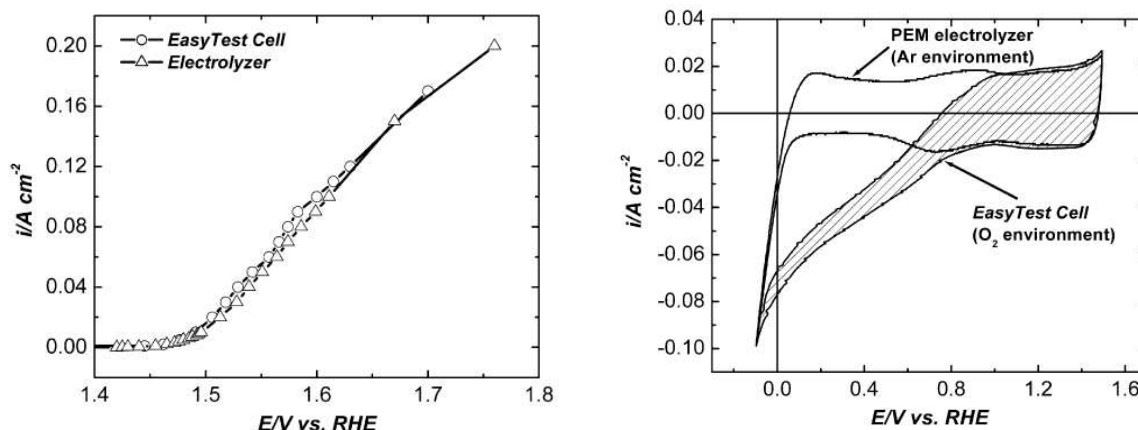


Figure 11: Comparison of the steady state polarization curves towards OER obtained in the EasyTest Cell and PEMWE at 20°C and 100% relative humidity (left) ; Cyclic voltammetry curves of the IrOx/Pt/IrOx electrode obtained in the EasyTest Cell and PEMWE at 20°C (right).<sup>[40]</sup>

Results show a quite good correlation between polarization curves obtained on the Easy Test Cell and on PEMWE, however cyclic voltammetry is distorted because of oxygen reduction reaction.

Advantage	Disadvantage
<ul style="list-style-type: none"> <li>- one reaction (except reverse reaction)</li> <li>- low internal resistance</li> <li>- experiments in condition representative of real application (pressure, temperature)</li> </ul>	<ul style="list-style-type: none"> <li>- MEA testing</li> <li>- CV impossible</li> </ul>



### III.3.3 Small size electrolysis cell

- Principle:

A small size electrolysis cell (typically 5 to 25cm<sup>2</sup>) can be used to evaluate the performance of the catalysts while using a small amount of catalyst. A full membrane – electrodes assembly has to be produced (including anodic and cathodic catalysts).

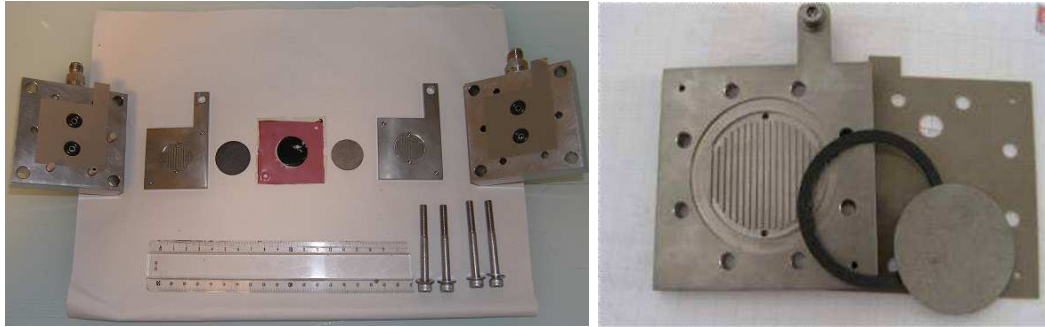


Figure 12 : 5 and 25 cm<sup>2</sup> single cells used for water electrolysis MEA testing

- Sample preparation: same as before, see [MEA preparation](#)

A suspension of catalyst in a mixture of solvent and binder is deposited on the membrane (spray, knife coating, screen-printing, decal ...) or on the gas diffusion layer. It is also possible to evaluate the influence of catalyst layer composition (amount of Nafion) and differences relative to the deposition technique.

Advantage	Disadvantage
- Real MEA testing - Small amount of catalyst needed	- MEA preparation (numerous parameters to take into account during assembly processes).

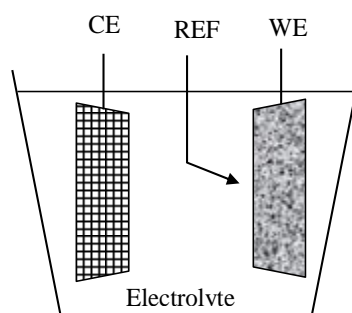


## IV. Testing protocols

To compare the results of tests conducted by NEXPEL partners on catalysts and MEA, it is necessary to harmonize the testing procedures and conditions under which these tests will be conducted. The aim of this paper is to describe the main tests and propose a detailed description of protocols.

### IV.1 Three electrode cell setup

The standard conditions for three electrode cell measurements (flat or rotating electrode) to characterize the NEXPEL catalysts are given in the table below.



Reference electrode	Reversible hydrogen electrode
Counter electrode	Platinum mesh or foil
Electrolyte	Sulphuric acid, 0.5 M made from p.a grade conc. H <sub>2</sub> SO <sub>4</sub> and ion exchanged water (18.2 MΩ).
Temperature	Standard: Room temperature (20-25°C) Elevated temperatures (up to 60 °C) can sometimes be used.



## ***IV.2 Sample preparation***

### ***IV.2.1 Deposition of catalyst suspension***

Aqueous suspensions of the catalyst materials are produced by ultrasonically dispersing the appropriate amount of catalyst in a mixture of 20% isopropanol in water. The amount of catalyst added is dependent on the loading of active material and also the density and surface area of the support.

Typically a 20  $\mu$ l aliquot of the suspension is pipetted onto the substrate. After evaporation of the water under flowing nitrogen atmosphere, 20  $\mu$ l of a diluted Nafion solution (1/100 5wt.% Nafion in pure water) is added on the top of the dried catalyst powder.

### ***IV.2.2 Catalyst ink***

The catalyst suspension is obtained, dispersing the catalyst powder with deionised water, isopropanol (20%) and Nafion (5wt.% solution). Amount of ionomer for standard test is fixed at 30wt.% for both anodic and cathodic catalysts.

### ***IV.2.3 MEA***

Ink is obtained as previously described (. The powder of catalyst is usually mixed with Nafion ionomère in alcoholic solution. Standard electrodes will prepared spraying the catalyst ink onto a PTFE support then decal on Nafion 117 membrane by hot pressing 135°C, 4 MPa for 3 minutes.



### ***IV.3 Characterization techniques***

#### ***IV.3.1 Cyclic voltammetry – Active surface Area***

For anodic catalysts, cyclic voltammetry would be performed between 0 and 1.4 V vs. RHE at 20 mV s<sup>-1</sup> under nitrogen bubbling.

Active surface area could be evaluated by measuring anodic and cathodic charge during voltammetry. The real EAS could be measured by Zn<sup>2+</sup> adsorption technique:

- Immersion of sample in a solution of 0.5M NH<sub>4</sub>Cl and 0.001M ZnO at room temperature
- After 16h, titration of the solution with 0.00025M EDTA using Erichrome Black T as an indicator.

Assuming an area of 1.7 nm<sup>2</sup> per adsorbed Zn<sup>2+</sup> ion, the EAS of the electrode is then calculated.

#### ***IV.3.2 Cyclic Voltammetry - Polarisation curves***

For anodic catalysts, cyclic voltammetry can be performed between 1.2 and 1.5 V/RHE on rotating disk electrode and between 1.2 and 1.7 V/RHE on half-cell. Slow scanning speeds (typically 1mV.s<sup>-1</sup> or 5 mV.s<sup>-1</sup>) are preferred to limit the effects related to capacitive phenomena.

On rotating ring disc electrode and half cell, the faradaic currents ( $I_f$ ) are relatively low and the contribution of capacitive current ( $I_c$ ) cannot be neglected. One way to reduce the capacitive effect is to reduce the scan speed to approach the steady state and limit the effects related to phenomenon of "charge / discharge the double layer" and pseudo capacitance. Figure 13 show the general shape of the voltammograms obtained for the water electro oxidation when tested in rotating disk electrode.

The black curve represents the response usually obtained for scanning between 1.18 and 1.53 V/RHE. For potentials lower than 1.35V / RHE, the electro oxidation reaction of water is not initiated and only the capacitive contribution is  $I_c$  present. To determine the onset potential of reaction ( $E(I = 0)$ ), characteristic of catalyst studied, it is necessary to overcome the capacitive part of the current.



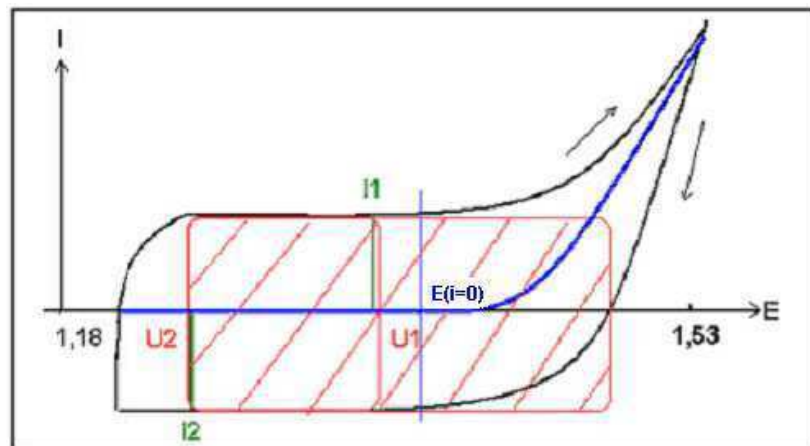


Figure 13 : Faradaic and capacitive currents measured during voltammetry

The crosshatched in red is subtracted to the black curve to obtain the blue curve corresponding at a first approximation to the faradaic current. It is then possible to determine the value of  $E (I = 0)$  or directly by plotting  $\log |j|$  vs.  $E$  (Tafel curves).

To subtract the capacitive effect, a fixed range of potential ( $U_1, U_2$ ), is used to determine the current values  $I_1$  and  $I_2$  corresponding respectively capacitive currents of the positive and negative sweep of the voltammogram. It is necessary to determine  $I_1$  and  $I_2$  as these two values are not always equal.  $I_1$  is sometimes more important than  $I_2$ , it may be due, for example, to a difference between adsorption and desorption of water from the catalyst.

The specific capacity of the sample can then be calculated as follows:

$$C_s = \frac{Q}{\Delta U} = \frac{I_1 + I_2}{V_b}$$

$I_1$  and  $I_2$  are expressed in A.

$V_b$  is the scanning speed  $V.s^{-1}$ .

$C_s$  is expressed in F.

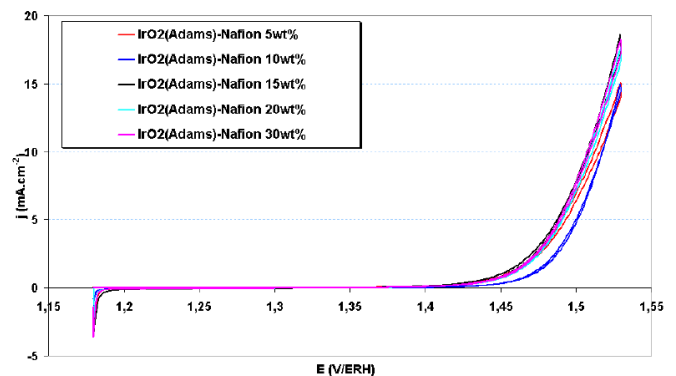
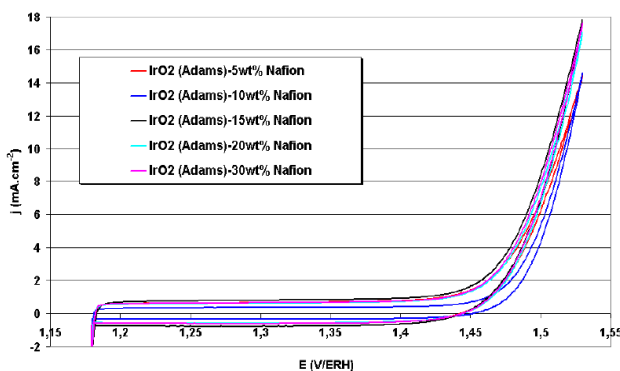


Figure 14 : CV curves before (left) and after (right) correction of capacitive effect





It is however still very difficult to determine accurately the potential  $E_{(i=0)}$ . Then we use "arbitrary" values that allow a consistent and more relevant interpretation:

- **E at  $-0.1\text{mA}\cdot\text{cm}^{-2}$** ; this value provides a comparison of potential more reliably the potential to which the reaction begins. The potential values are taken at the scan to negative potentials.

- **j at 1.5 V/RHE**; Comparison of current densities for low voltage. The current density values are also read from the scan to the potential negative.

	$C_s$ (F)	$R_\Omega$ ( $\Omega$ )	E (V vs RHE) at $0.1\text{mA}\cdot\text{cm}^{-2}$	j ( $\text{mA}\cdot\text{cm}^{-2}$ ) at 1.5V vs. RHE
Catalyst 1	0.18	6.7	1.414	12.2
Catalyst 2	0.17	6.9	1.431	12.4
Catalyst x	...	...	...	...

**Table 1** : example of values determined on catalyst



#### IV.4 Impedance spectroscopy measurements

The frequency range typically used for impedance spectroscopy characterization of PEM electrolysis MEAs is generally comprised between a few tens of kHz and several hundred MHz.

Depending on the equipment used, it is possible to apply a current or a voltage signal. The amplitudes of the signals can be highly variable, but mainly for measurements of impedance spectroscopy to observe the following conditions:

- Linear response over a solicitation (user refines  $U = f(j)$ )
- Stationary (not changing the system over time)

It is essential to define accurately the frequency range, the type of solicitation electrical (current or voltage) and the amplitude of the signal.

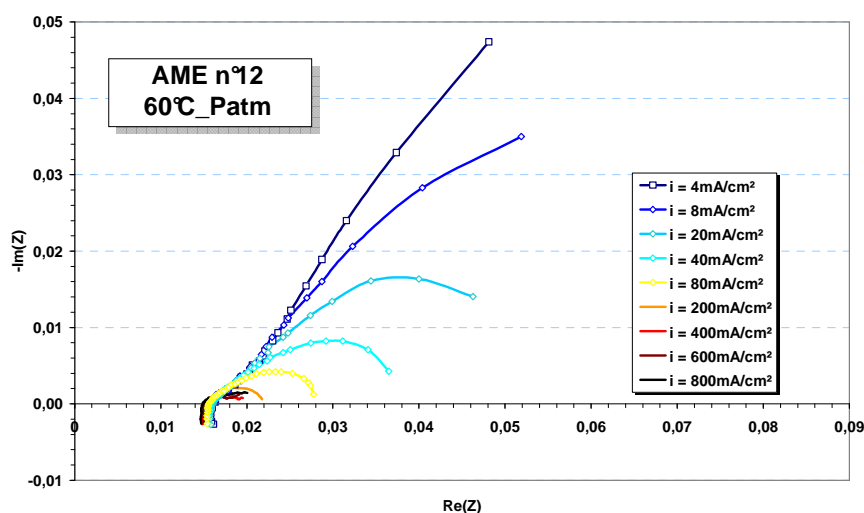


Figure 16 : impedance spectroscopy measurements on a PEM-WE MEA at various current densities

A special attention should be paid to the electrical connections of the device with the system under study. It will obviously minimize the potential sources of capacitive and inductive phenomena (connexions, crocodile clips, length of electrical wires, etc ...).

Measurements of electrochemical impedance spectroscopy are generally also performed on rotating ring disc electrode and half cell to evaluate the ohmic resistance of the system and the charge transfer resistance. The frequency range of study is 200 kHz - 100 mHz and the amplitude peak to peak of 10 mV. It is interesting to make these measurements different points of the polarization curve.



#### ***IV.5 Stability criteria (half cell and single cell tests)***

The stability conditions at an operating point should verify the following criteria:

- 1 - Stability of pressure ( $\Delta P < 10\%$  pressure) over a period of 2 minutes
- 2 - Stability of gas flow rates ( $\Delta Q < 1\%$  rate) over a period of 2 minutes
- 3 - Stability of the amount of hydrogen in oxygen and oxygen levels in hydrogen ( $\Delta \tau < 0.1\%$ )
- 4 - Stability of temperature ( $\Delta T < 2^\circ\text{C}$ ) over a period of 2 minutes
- 5 - Voltage stability ( $\Delta U < 5\text{mV}$ ) over a period of 2 minutes

- Procedure:

- After applying a stabilized current density, observation of pressure, flow and temperature variation versus time (2 min).
- If the parameters are stable ( $\Delta P < 10\%$ ,  $\Delta Q < 1\%$ ,  $\Delta \tau < 0.1\%$ ,  $\Delta T < 2^\circ\text{C}$ ), the voltage is considered stable when the voltage variation is less than  $\pm 5\text{mV}/\text{cellule}$  on the period of 2 minutes.
- In case of oscillations, measure the oscillation frequency and the average value of at least 3 periods. Voltage is considered stable when changing the voltage is below where  $5\text{mV}/\text{cellule}$  on the period of 2 minutes.



#### IV.6 Polarisation curve (single cell tests)

This procedure must be followed to record a polarization curve.

1- The cell must operate at fixed conditions (current, pressure, temperature, etc...) for at least 30 minutes and verify the following criteria:

- Stability of pressure, gas flow, purity, temperature during the last 2 minutes
- Stability of cell tension  $< \pm 5\text{mV}$  over 2 minutes

2- Polarization curve begins after stabilization of current density at  $1\text{ A cm}^{-2}$ .

3- The current is then increased to  $2\text{ A cm}^{-2}$  by steps of  $0.2\text{ A cm}^{-2}$ , 2 minutes long.

- The current increase will be restricted if the cell voltage reaches  $2.5\text{V}$ . Then, the maximum current density  $j_{\text{max}}$  will be defined.

4- Current is then stabilized at the maximum current density ( $j_{\text{max}}$ ) for 2 minutes, verifying stability criteria next reduced by steps of  $0.2\text{ A cm}^{-2}$  still verifying stability criteria.

- It is important to note  $\tau_{\text{H}_2}$  and  $\tau_{\text{O}_2}$ . When reaching the highest value of safety (1%), decreasing current steps are interrupted. The current density then correspond to the minimum current of system operation in these conditions:  $j_{\text{min}}$

5- If possible, a step at  $0.1\text{ A cm}^{-2}$  stabilized will be realized.

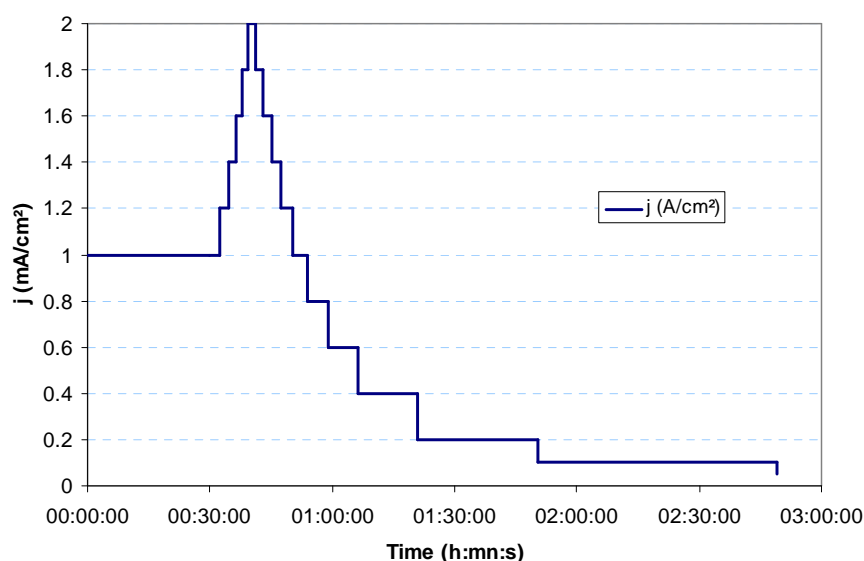


Figure 17 : example of proposed protocol for polarization curve recording

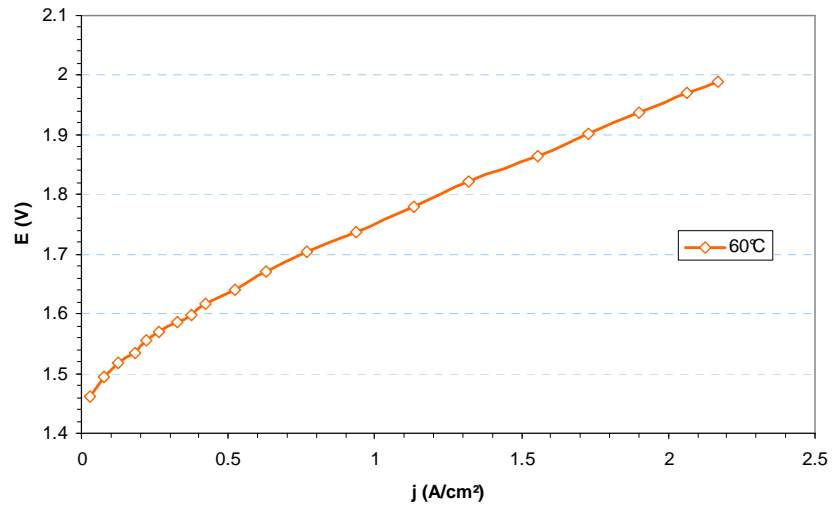


Figure 18 : example of polarization curve

	E (V) at 1A/cm <sup>2</sup>	R <sub>Ω</sub> (mΩ.cm <sup>2</sup> )	j <sub>max</sub> (A.cm <sup>-2</sup> )	j <sub>min</sub> (A.cm <sup>-2</sup> )	τ <sub>H<sub>2</sub></sub> (%) at 1A.cm <sup>-2</sup>	τ <sub>O<sub>2</sub></sub> (%) at 1A.cm <sup>-2</sup>
MEA 1 (60°C, P <sub>atm</sub> )	1.73	0.175	-	0.1	0.8	0.5
MEA 2 (T°C, P)	1.82	0.205	1.75	0.1	0.6	0.4
MEA X (T°C, P)	...		...	...	...	

Table 6: example of table showing the main performance results



## V. References

---

- <sup>1</sup> S. Grigoriev et al. WHEC 16 / 13-16 june 2006 Lyon
- <sup>2</sup> J. Wu et al, International journal of hydrogen (2008), vol. 33, no6, pp. 1735-1746
- <sup>3</sup> T. Vidakovic et al. Electrochimica Acta 52 (2007) 5606-5613
- <sup>4</sup> A. Lasia Journal of Electroanalytical Chemistry 562 (2004) 23-31
- <sup>5</sup> A. Lasia, Journal of Electroanalytical Chemistry 593 (2006) 159-166
- <sup>6</sup> H. Ducnan Journal of Electroanalytical Chemistry 621 (2008) 62-68
- <sup>7</sup> X. Xue et al., Electrochimica Acta 50 (2005) 3470–3478
- <sup>8</sup> F. Maillard et al, Faraday Discuss. (2004), 125, 357-377
- <sup>9</sup> A. Pozio et al. Journal of Power Sources Volume 105, Issue 1, (2002) 13-19
- <sup>10</sup> F. Maillard et al. Journal of Electroanalytical Chemistry 599 (2007) 221-232
- <sup>11</sup> F. Delime et al. Journal of Applied Electrochemistry 28 (1998) 27-35
- <sup>12</sup> H. A. Gasteiger et al., Journal of Physical Chemistry, Vol. 97, No. 46, 1993
- <sup>13</sup> K.A. Soliman et al., Electrochemistry Communications 11 (2009) 31–33
- <sup>14</sup> E. Rasten, Doctor Engineer thesis, Norwegian University of Science and Technology, october 2001
- <sup>15</sup> F. Mattos-Costa et al., Electrochimica Acta 44 (1998) 1515-1523
- <sup>16</sup> C.P. De Pauli et al. Journal of Electroanalytical Chemistry 396 (1995) 161-168
- <sup>17</sup> A. Marshall et al., Electrochimica Acta 51 (2006) 3161–3167
- <sup>18</sup> J. Gaudet et al. Chem. Mater., Vol. 17, No. 6 (2005) 1570-1579
- <sup>19</sup> A. Kozawa, J. Inorg. Nucl. Chem., 21, (1961) 315
- <sup>20</sup> W. O'Grady et al., in "Electrocatalysis," M. W. Breiter, Editor, p. 286, The Electrochemical Society Softbound Proceedings Series, Princeton, NJ (1974).
- <sup>21</sup> R.F. Savinell et al. J. Electrochem. Soc., Vol. 137, No. 2, (1990) 489-494
- <sup>22</sup> L. D. Burke and O. J. Murphy, J. Electroanal. Chem., 96 (1979) 19
- <sup>23</sup> K.C. Neyerlin et al. Journal of The Electrochemical Society, 156 (3) (2009) B363-B369
- <sup>24</sup> R. Forgie et al. Electrochemical and Solid-State Letters, 13 (4) (2010) B36-B39
- <sup>25</sup> L.F. Petrik et al., Journal of Power Sources 185 (2008) 838–845
- <sup>26</sup> A.T. Marshall, Electrochimica Acta 55 (2010) 1978–1984
- <sup>27</sup> X. Cui et al., Materials Chemistry and Physics 113 (2009) 314–321
- <sup>28</sup> R. Balaji et al., Electrochemistry Communications 11 (2009) 1700–1702
- <sup>29</sup> P. Millet et al. Int. Journal of Hydrogen Energy 35 (2010) 5043
- <sup>30</sup> X.-M. Wang et al., Electrochimica Acta 55 (2010) 4587–4593
- <sup>31</sup> F. Ye et al. Int. Journal of Hydrogen Energy 35 (2010) 8049
- <sup>32</sup> C.R. Costa et al., Journal of Hazardous Materials 153 (2008) 616–627
- <sup>33</sup> D. Profeti et al. J Appl Electrochem 38 (2008) 837–843
- <sup>34</sup> A.M. Mohammad et al., Electrochimica Acta 53 (2008) 4351–4358



- <sup>35</sup> M. Yagi et al. J. Phys. Chem. B, Vol. 109, No. 46, (2005) 21489-21491
- <sup>36</sup> S. Tong et al., Chinese Journal of Chemical Engineering, 16(6) (2008) 885-889
- <sup>37</sup> A. Habibi et al. Int. Journal of Hydrogen Energy 33 (2008) 2668
- <sup>38</sup> A. Marshall et al., Energy 32 (2007) 431–436
- <sup>39</sup> U. Wittstadt et al., Journal of Power Sources 145 (2005) 555–562
- <sup>40</sup> G. Wei et al. Int. Journal of Hydrogen Energy 35 (2010) 3951
- <sup>41</sup> A.T. Marshall et al., Int. Journal of Hydrogen Energy 33 (2008) 4649
- <sup>42</sup> S. Grigoriev et al., Int. Journal of Hydrogen Energy 34 (2009) 4968
- <sup>43</sup> E. Rasten et al., Electrochimica Acta 48 (2003) 3945-3952
- <sup>44</sup> S. Song et al., Electrochemistry Communications 8 (2006) 399–405
- <sup>45</sup> S. Song et al. Int. Journal of Hydrogen Energy 33 (2008) 4955– 4961
- <sup>46</sup> L. Ma et al., Int. Journal of Hydrogen Energy 34 (2009) 678
- <sup>47</sup> S. Siracusano et al., Electrochimica Acta 54 (2009) 6292–6299
- <sup>48</sup> S. siracusano et al., Int. Journal of Hydrogen Energy 35 (2010) 5558-5568
- <sup>49</sup> V. Antonucci et al., Electrochimica Acta 53 (2008) 7350–7356
- <sup>50</sup> S. Zhigang et al., Journal of Power Sources 79 (1999) 82–85
- <sup>51</sup> T. Ioroi et al., Journal of Power Sources 112 (2002) 583–587
- <sup>52</sup> I. Radev et al., Electrochimica Acta 54 (2009) 1269–1276